Quarterly Progress Report
For the period August 1, 1969 through January 31, 1970
NASA Contract NGR 44-004-030
Laboratory Studies of Plasma Probes

W. J. Heikkila
Principal Investigator

* * * * *

W. D. Bunting, Jr. - Co-investigator
J. Tarstrup - Co-investigator

Continued progress is being made in the theoretical interpretation of our experimental data. Two publications have been written so far and one of them has been accepted by the Journal of Applied Physics to be published in April, 1970 issue. A70-31765 The other one had just been submitted to Radio Science and will hopefully be published shortly. Both publications are included with this report. A72-26768

A 70-31765

Observations on the Effect of Surface Conditions on Langmuir Probes

W. D. Bunting, Jr.

and

W. J. Heikkila

The University of Texas at Dallas

Dallas, Texas

Submitted to

Journal of Applied Physics

November, 1969

ABSTRACT

Langmuir characteristics have been recorded for probes having various surface conditions. The measurements are made in a plasma which has an electron density and electron temperature characteristic of the ionosphere. It is shown that reliable probe measurements are obtained only when the probe surface is carefully cleaned; in this case the method found most successul is a discharge cleaning which sputters off the contaminants.

Observations on the Effect of Surface Conditions on Langmuir Probes

W. D. Bunting, Jr.

and

W. J. Heikkila

The University of Texas at Dallas

Dallas, Texas

Langmuir probes have been used widely to measure electron density N_e and temperature T_e in laboratory and ionospheric plasmas. We have observed that probe surface conditions are very important in low density, low temperature ($N_e < 10^7$ cm^{-3}, $T_e < 10^3$ °K) conditions such as are characteristic of the ionospheric plasma. It seems that errors are caused by variations of the work function over the probe surface and by insulating layers such as oxides or hydrocarbons. Evidence of similar problems in higher density and hotter laboratory plasmas has been discussed by Wehner and Medicus[1] and more recently by Kostelnicek.[2] The purpose of this communication is to show that reliable Langmuir probe measurements can be obtained if the probe surface is carefully cleaned. The method found most successful is a discharge cleaning which sputters off the contaminants.

The plasma used for this experiment was produced by a cold cathode discharge in nitrogen at a pressure of 0.15 torr. The containing chamber was a 30 inch long, 20 inch diameter, stainless

steel cylinder. A discharge was maintained in each of two bell jars, one on each end of the cylinder. With this arrangement the electron gas is cooled by collisions as it diffuses through the neutral gas to the experiment area in the center of the chamber.

The principles and theory of the Langmuir probe are well known so that they need not be discussed here. In this experiment the probe was a 0.5 centimeter diameter, gold plated, stainless steel sphere. The logarithm of the absolute value of the probe current was displayed as a function of probe potential on an oscilloscope. A triangular voltage sweep was applied to the probe (with the chamber wall as zero reference) and the logarithm of the current was recorded both as the potential was increasing and as it was decreasing. The total time for one complete recording was one second.

Some results of the experiment are shown in Figure 1. The plasma conditions were measured by a separate clean probe; in each case the plasma parameters had approximately the values $N_e = 8 \times 10^6$ cm^{-3} and $T_e = 400°K$. The small arrows indicate the direction in which the oscilloscope spot was moving along the recording.

Figure 1 (a) shows a Langmuir characteristic for an uncleaned probe, that is, nothing had been done to the probe surface after it was gold plated. Figure 1 (b) shows the characteristic after the probe had been cleaned with trichlorethylene, acetone, and methanol in that order. Figure 1 (c) shows the characteristic after the probe had been discharge cleaned by applying a negative potential of 2000

volts to the probe while it was in nitrogen at a pressure of 0.03 torr; the potential was applied for approximately one minute.

It is at once obvious that repeatable plasma measurements are provided only by the probe which had been discharge cleaned. The long semi-logarithmic part of its characteristic is normal for the electron retarding region, and its slope gives a good value for the temperature (T_e = 400°K), and the break point identifies the space potential and hence electron density (V_s = 0.11 volts, N_e = 8.2 x 10^6 cm^{-3}).

The dirty probes are subject to several defects. Non-repeatability is demonstrated by the open loop in the retraced characteristic. This will be called hysteresis although the current leads rather then lags the voltage. The amount of hysteresis increases with the total time taken to retrace the characteristic. Under d.c. conditions the effect shows up as a slow drift in the probe current when the probe potential is held at a constant bias. The amount of hysteresis also increases with increasing bias voltage amplitude. Chemical cleaning helps slightly. Discharge cleaning for at least some tens of seconds is usually adequate for a good probe with uniform surface, but if the probe is then exposed to the atmosphere, the characteristic again exhibits hysteresis, the amount depending upon the length of time exposed and the atmospheric conditions. Finally, if the probe is discharge cleaned for an excessively long time the gold plating becomes thin (appearing

lighter in color), or it may even be removed, and the shape of the characteristic is badly altered. No hysteresis is observed in this case and the characteristic may have a straight line portion on a semilogarithmic plot but the length of this portion is short and its slope is greatly decreased from that of Figure 1 (c).

Other defects evident in Figure 1 (a) and (b) include a reduction in electron current, a shift in floating potential (i.e., potential for which no current is collected), and lack of a good straight line in the semilogarithmic characteristic. Sometimes a straight portion can be selected but usually its slope is too small, thus providing too high an estimate for electron temperature.

Although we have not attempted to explain these observations in detail, we believe that they could be caused by a thin insulating layer on the probe surface. Such a layer might be formed simply by adsorbed gases, or by other contaminants picked up by contact. The effect would be to form a leaky capacitor in series with the probe. In practice, the lesson on the use of the Langmuir probe as a diagnostic tool is clear.

We wish to acknowledge that this work was supported by NASA grant NGR44-004-030.

vii

References

[1]G. Wehner and G. Medicus, J. Appl. Phys. 23, 1035 (1952).

[2]R. J. Kostelnicek, Aeronomy Report No. 8, Department of Electrical Engineering, University of Illinois (1965).

Figure Captions

Figure 1. Langmuir characteristics for (a) uncleaned probe (b) chemically cleaned probe and (c) discharge cleaned probe. Plasma conditions are: $N_e = 8 \times 10^6$ cm^{-3}, $T_e = 400°K$, pressure = 0.15 torr.

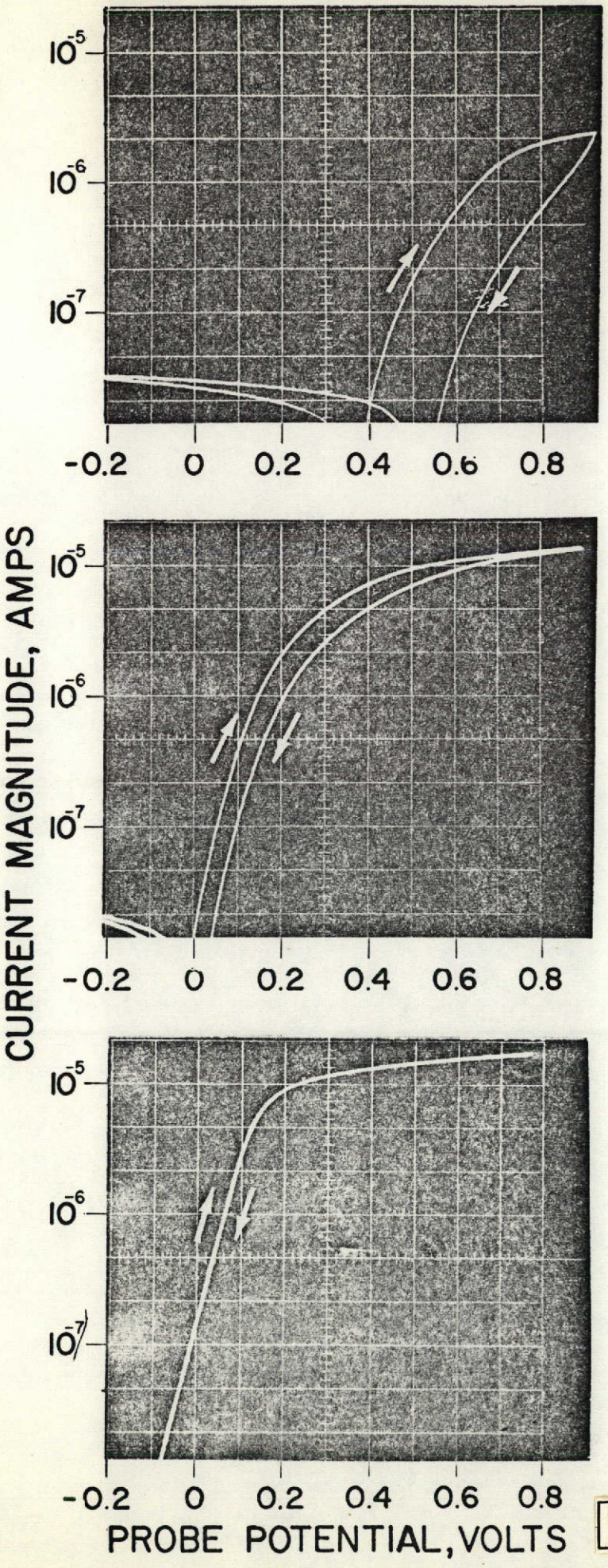

(a)

(b)

(c)

Observations of the Impedance Characteristic of a Spherical Probe as a Function of Probe Potential

by

Jens Tarstrup
The University of Texas at Dallas
Dallas, Texas

ABSTRACT

An accurate experimental technique for measurement of the complex impedance of a spherical probe in a weakly ionized gas is described. Guarded hemispheres were used to obtain a purely radial electric field; the diameters were in the range from 7 to 20 millimeters (~10-30 Debye lengths). The plasma frequency was of the order of 15 MHz, and the electron collision frequency about 1/10 of that. Both the real and imaginary part of the impedance showed a resonant behavior near the plasma frequency, with details depending on the electron temperature and collision frequency as well as probe potential. A 7% shift of the frequency where the real part peaks was observed when the probe potential was changed from floating potential to space potential. Theoretical results based on a hydrodynamic model of the plasma, with a simple vacuum sheath surrounding the probe at floating potential, do not predict any such frequency shift.

1. Introduction

The small signal impedance of a radio-frequency probe in a warm plasma has been discussed by several authors. Many different probe geometries have been used such as parallel plates, cylindrical dipoles, co-axial lines, slotted spheres, spheres, etc. We will concentrate this treatment on the impedance characteristic of a spherical probe. In a spherical geometry, the current density supplied by the plasma goes down faster than for any other configuration, and can be neglected far away from the probe, which is better for both experiment and theory. In constructing theoretical models, it is therefore reasonable to assume that an isotropic Maxwellian electron velocity distribution is established at large radial distances maintained by collisions.

The purpose of this work was to measure the spherical probe impedance characteristic in a plasma, to compare experimental results with the different theories available and to establish the true unperturbed electron density in the plasma.

Crawford and Harp (1964-65) has published a series of papers, where the spherical probe impedance characteristic and resonance probe characteristic were discussed. For small collision frequencies they performed experiments where a RF signal was applied to a probe immersed in a plasma and a DC resonance was observed. They were able to calculate from their theory the ratio between the resonance frequency and the plasma frequency and confirm their results with other experimental measurements. They found too that

a parallel resonance occurred at the plasma frequency, although the resonance was so broad that the frequency was difficult to define.

To the author's knowledge, the few reported experimental impedance measurements have been partly in error because of the electric field perturbation caused by the necessary electric connection to the probe under test. This effect was to some extent reduced in the results described here, by performing the measurements on guarded hemispheres as explained in Section 2. It was verified that the impedance characteristic of a sphere located at the same place in the plasma as a guarded hemisphere had deviations by a factor of two in both the real and imaginary parts at certain frequencies. Particular attention was directed to obtain accurate and repeatable results so that a meaningful test of the theories could be attempted. The measurements appear to reveal inadequacies in all of the theoretical models except the one by Buckley (1967), as far as establishing the correct electron density.

2. Experimental Technique

The vacuum chamber pictured in Figure 1 was used for the experimental studies. This system included a small roughing pump and a 5 cm air-cooled diffusion pump with a liquid nitrogen baffle. The belljar had a 35 cm diameter and rested on a chrome plated brass base. The plasma was produced by a cold cathode glow discharge with the geometry and location shown in Figure 1. Since

a low electron density was required, ($\sim 10^7$ electrons cm^{-3}) a single stainless steel rod about 12 cm long and 6 mm in diameter was sufficient as a cathode. In order to shield the region near the probe from the ultraviolet radiation and energetic electrons produced by the discharge, a baffle was installed above the cathode, as shown. The system was continuously pumped, with fresh gas admitted through a needle valve. The measurements reported here were taken in nitrogen at pressures between 15 and 50 microns. A discharge current of the order of 1 mA at a cathode voltage of minus 1000 V was required to produce a plasma with a density $N \simeq 3 \times 10^6$ electrons cm^{-3} at 40 microns Hg.

The measurements were performed with split spherical probes made of stainless steel (Figure 2). The upper hemisphere was the test probe, and was connected to the center wire of a tri-axial cable. The lower hemisphere was used as a guard electrode, and was connected to the inner cylindrical shield. Finally, the outer cylindrical shield was grounded at the connector and cut-off close to the lower hemisphere, thereby shielding the plasma from large perturbations from the cable. The guard probe was held at very nearly the same DC and RF potential as the test probe during the measurements; in this way the perturbation introduced by the connecting lead did not disturb the field of the top hemisphere, which then closely approximated half of the isolated sphere always assumed in the theoretical work.

A block diagram of the instrumentation used to measure the impedance characteristic is shown in Figure 3. It was found that the plasma potential in the volume under test would follow the potential of the outer sphere (screen), representing infinity. However, it was also found that another probe, called the reference probe, would have nearly the same floating potential as the test probe after a proper cleaning by ion bombardment. It could, therefore, be used as a reference and Figure 3 shows a servo loop with the object of holding the floating potential of the test probe at ground potential during the measurements. This was a convenient reference when the probe bias was changed to space potential.

The impedance of the probe was measured by the following procedure: The oscillator was connected to the screen through a suitable network, thereby exciting the plasma far away from the probe. The screen was fed from a 5 ohms source, so that the voltage on it was independent of loading by the plasma. Because the screen is an equipotential surface, the electric field is purely radial. The total current through the top hemisphere is represented by the voltage across C_L. Two identical pre-amplifiers with Field-Effect transistor input circuitry were developed to measure the voltage on the probe and on the screen. The probe voltage was measured across C_L which was several orders of magnitude larger than the free space probe capacitance. These two voltages were measured in amplitude and phase on a Hewlett Packard sweep

generator and phase/amplitude tracking detector model 675/676A, with a sweep frequency of 10 Hz.

The output data, in the form of an amplitude and a phase response of the probe impedance, were shown instantaneously on an oscilloscope, thereby permitting a Polaroid picture to be taken for each experiment. A typical response with and without plasma in the vacuum chamber is shown in Figure 4, where the difference between the two sets of curves is, in effect, a normalization of the amplitude/phase response. Frequency markers from 1 to 21 MHz have been inserted to calibrate the abscissa, and each vertical division corresponds to 2 DB or 10°. A scaling was performed on many such Polaroid pictures to calculate the normalized real and imaginary part of the impedance characteristic. The error in using the outer sphere (screen) as infinity introduced an increase of 4% in the free space capacity, but by normalizing the experimental results it is shown in Appendix 1 that this error is almost cancelled out.

The error in measuring the impedance characteristic is as follows. The amplitude response can be measured with an accuracy of $\pm$ 0.2 DB which for a 3 DB deviation from the free space response corresponds to a $\pm$ 4% error. The phase response can be measured with an accuracy of $\pm$ 1°, which for phase angles larger than 20° from the free space response corresponds to an error of less than 4%. Since the experimental points can be smoothed out by

a curve fitting technique, it is estimated that the normalized impedance characteristic is known within ± 4% over most of the frequency range.

No account has been taken of the effect of the magnetic field (<0.5 gauss). Crawford and Harp (1965) have made some estimates of the magnetic field effect. It was our experimental observation that no correction was necessary for the electron density and temperature used in this work, since a field increase to 2 gauss did not alter the impedance characteristic significantly.

3. Experimental Results

A factor which will affect the impedance is the uniformity of the electron density, particularly in the vicinity of the probe. Figure 5 shows such a profile taken in the horizontal and vertical plane of the vacuum system by Langmuir probe techniques. The density variation was almost parabolic. Most theories presume a uniform electron density to infinity, but it is shown in Appendix 1 that the above profile gives an adequate sampling volume for a 1 cm spherical probe. The electron temperature has been measured extensively by Langmuir probes and the results are reported by Bunting (1968). It was found that the electron temperature varied from 300° to 500° K based upon the exponential portion of a Langmuir curve, but a high energy tail often appeared on the trace, dependent upon the pressure and electron density. It is assumed for the discussion later that the electron temperature was 350°K, in other words close to the neutral temperature, since the bulk of the plasma was at that low temperature.

Many experiments were performed to measure the impedance characteristic at floating potential and at space potential in the same plasma. Using the instrumentation described in Section 2, it was possible to go back and forth between measurements in 10 seconds and verify that the results were repeatable and the plasma was stable. Figure 6 shows a typical recording of both the real and imaginary part of a 1 cm probe at floating potential and at space potential. The latter potential was established by measuring the DC current I_p, to the probe during a test, and from the knowledge of Te = 350°K. It was also necessary to know the electron density N, since from Langmuir probe theory

$$J_p = eN \frac{\sqrt{kTe}}{2\pi m}$$

e = electron charge
m = electron mass
k = Boltzmann's constant

at space potential, but from the analysis in Section 4, the plasma frequency was found to be fairly close to f_r, the frequency where the real part peaks. A quicker way of determining the space potential experimentally was simply to observe the amplitude/phase characteristic on the oscillograph during a bias change. As the potential on the probe was raised from floating potential to space potential, the impedance characteristic varied until space potential was reached (sheath collapsed). After that no more change could be observed, at least until the current to the probe was a factor of about two times that at space potential.

A careful analysis of all the experiments performed as above shows an increase of f_r going from floating potential to space

potential. This frequency was identifiable within $\pm 2\%$ and Table 1 gives a summary of the results. It will be noted that the average frequency shift of f_r is seven percent. This will be discussed in the next section.

4. Comparison of Experimental Results with Theory

Fejer (1964) has computed the impedance characteristic using a hydrodynamic approach at floating potential, assuming a perfectly reflecting probe/plasma boundary. Balmain (1966) also used a hydrodynamic approach in calculating the impedance at plasma potential, assuming the sheath to be completely collapsed, and a total electron absorption by the probe. This work has been extended by Holt (1965-67) and Kostelnicek (1965) to include electron neutral collisions and a vacuum sheath. For a probe at floating potential, assuming a vacuum sheath surrounding the probe, the impedance will consist of two parts in series, a capacitive contribution from the sheath and a plasma part. Using a hydrodynamic approach in the plasma outside the sheath, assuming constant electron density, the following equations must be satisfied: Momentum transfer equation representing conservation of momentum

$$mN \frac{\partial \bar{v}}{\partial t} = Ne \nabla V - \gamma kT \nabla n - \upsilon mN\bar{v}$$

The force is equal to the sum of the contributions from the electric field, pressure and friction. Continuity equation stating conservation of charge

$$\nabla \cdot (N\bar{v}) = - \frac{\partial n}{\partial t}$$

Poisson's equation for effect of charge separation

$$\nabla^2 V = \frac{e}{\epsilon_o} n$$

The symbols are explained in Appendix 3. Using Balmain's (1966) terminology, the following expression can be derived for the impedance of the plasma part (his equation 49)

$$Z_{p1} = \frac{1}{j\omega 4\pi(r_o + s)\epsilon_o K_o} \left[1 - \frac{X}{U}(1 + \alpha_1\rho' - jaX^{1/2}\alpha_1^2\rho')^{-1}\right]$$

The ratio of the specific heat γ enters the computation through α_1. The variation of γ over the frequency range has been calculated by Pavkovich (1964) on the basis of kinetic theory, and a linear approximation from $\gamma = 1$ at $f = 0.1 \times f_N$ to $\gamma = 3$ at $f = f_N$ has been used in our computations. The total probe impedance is then equal to $Z_{\text{probe 1}} = Z_{\text{sheath}} + Z_{p1}$. A particular combination of plasma-probe parameters relevant to our experimental data has been assumed in the computation and the result is plotted in Figure 7, to be compared with other results later.

A cold plasma approach will now be discussed where the medium is assumed to be a Lorentz plasma. For a probe at floating potential, assuming a vacuum sheath as before, the impedance of the plasma part is given by,

$$Z_{p2} = \frac{1}{j\omega 4\pi\epsilon_o} \int_{r_2}^{\infty} \frac{dr}{r^2 K_o} = \frac{1}{j\omega 4\pi\epsilon_o(1 - \frac{X}{U})\, r_2}$$

where $K_o = 1 - \frac{X}{U}$ is the cold plasma relative permittivity. The same combination of parameters as before has been used in the computation of Z_{p2}. The total probe impedance $Z_{\text{probe 2}} = Z_{\text{sheath}} +$

Z_{p2} is also shown in Figure 7. Two other results are included in the same graph using cold plasma approach in the transition region between the vacuum sheath and the plasma. A detailed calculation of this transition region is given in Appendix 1. It will be noticed that f_r occurs at the plasma frequency for all four cases and that the damping around plasma frequency is slightly larger for the hydrodynamic approach than for the cold plasma approach. It will also be noticed that the transition region, using cold plasma theory, does not alter the impedance characteristic significantly in the vicinity of the plasma frequency.

A kinetic theory model of the plasma has been used by Buckley (1967) to calculate the impedance characteristic at floating potential. He used the Boltzmann-Vlasov equation, together with Maxwell's equations, to derive an integral equation governing the alternating electric field in the plasma. The theoretical DC-sheath profile was taken from Bernstein and Rabinowitz (1959) for a collisionless plasma with mono-energetic electron distribution. Collisions between electrons and neutrals were included through a simple relaxation term in the Boltzmann equation. The integral equation was solved by a Matrix inversion technique,but the only published data were for a probe size of 5.2 λ_D. Figure 8 shows the impedance characteristic for two different collision frequencies from Buckley (1967) page 175. Also shown is the previously discussed impedance characteristic

using the hydrodynamic approach. It will be noticed that there are two significant differences. First, the damping of the resonance is about the same for a factor 3.5 in the collision frequency. This is qualitatively reasonable since Landau damping is included in this more exact treatment and contributes to the loss mechanism in the sheath. Second, and more important the whole characteristic is shifted down in frequency about 12% compared to the hydrodynamic approach. This is at first surprising but might possibly be explained by the electron density profile used in the hydrodynamic approach.

Figure 9 shows a theoretical fit of the experimental data for a 1 cm probe at floating potential using the hydrodynamic approach given above. The best fit was obtained for a Debye length λ_D, of 0.83 mm. ($\pm 5\%$), a sheath thickness of $4.3\lambda_D$($\pm 5\%$) and a collision frequency of $0.35 \times \omega_N$ ($\pm 10\%$). This corresponds to a probe size of $6\lambda_D$. The sheath thickness $s = 4.3\lambda_D$ as obtained approximates well to $s \sim 5\lambda_D$ measured by Crawford and Harp (1965) in some resonance rectification experiments, and to Mayer's experimental results, $s \sim 3\text{-}5\lambda_D$ (1963) from coaxial probes. Holt (1967) used the same basic concept as above to obtain the electron density profile of the ionosphere from an impedance characteristic experiment carried in a rocket.

The theoretical curve for the same 1 cm probe at space potential was used by letting s, the sheath thickness, go to zero in the same computer program. This result is also seen in Figure 9, where the theoretical curves are superimposed on the

experimental curves, so that f_r occurs at the same frequency for each comparison. The frequency shift of f_r cannot be explained using these theoretical models, since f_r, according to the computations, should occur at the plasma frequency for both cases.

To possibly explain this frequency shift, another calculation using the simple cold plasma theory has been done for a probe at space potential. This time the electron density was not assumed constant all the way to the probe surface, but depleted according to the following formula:

$$N = No \frac{r + \sqrt{r^2 - r^2}}{2r}$$

This equation was derived by Laframboise (1966) for a probe at space potential and corresponds to the geometric depletion factor due solely to the solid angle subtended by the probe, and is valid for a plasma which is not collision dominated. From the calculation performed, (Appendix 2), it was found that f_r occurred 5% below the plasma frequency.

5. Discussion

We now have the following facts to consider: According to Buckley's calculation for a probe at floating potential, f_r occurs 12% below the plasma frequency, and from above using a realistic electron density profile, although cold plasma theory, for a probe at space potential, f_r occurs 5% below the plasma frequency. The experimental data in Table 1 indicates an average frequency shift of f_r to be +7%, going from floating to space potential, basically same result as above. This seems to indicate, that the plasma frequency is probably 12% higher than f_r for a

probe at floating potential, or in other words, the electron density obtained before by the simple hydrodynamic/abrupt vacuum sheath model may be incorrect. The comparison shows also that the collision frequency obtained by the hydrodynamic approach is probably in error. An estimate from Buckley's calculation give $\chi = 0.1$, instead of $\chi = 0.35$ from Figure 9. This is a reasonable collision frequency too, because at a pressure of 30μ, at which the experiment was performed, a collision frequency of 7.5×10^6 sec^{-1} should be obtained according to Phelps and Pack (1959). Since the plasma frequency is about 16 MHz, $\upsilon = 0.1 \times 2\pi \times 16 \times 10^6 \propto 10^7$ sec^{-1}, which is within 25% instead of being off by a factor of 3-4.

6. Conclusions

Comparisons between experiment and theory have shown that a hydrodynamic model of the plasma with a simple vacuum sheath gives a good fit of the experimental data, but some of the obtained plasma parameters may be incorrect. It is concluded that the electron density obtained from the hydrodynamic model for a probe at floating potential should likely be increased by 25% corresponding to a plasma frequency increase of 12%. The actual electron-neutral collision frequency appears to be about 3 to 4 times larger than established by the hydrodynamic model. This last observation corresponds to collision frequencies obtained by resonance rectification experiments by Cairns (1963). A significant contribution to the understanding of a RF-probe at space potential could be made by using a kinetic theory approach as Buckley did

with a realistic electron density profile. This would hopefully verify the experimental observation of the frequency shift reported here.

ACKNOWLEDGMENT

It is a pleasure to thank Professor W. J. Heikkila for his guidance in this investigation, especially for his suggestion of using guarded hemispheres as test probes.

This work was conducted under NASA Contract NGR-44-004-030.

REFERENCES

Bachynski, M. P., "Source in unbounded plasmas," RCA Victor Research Report No. 7-801 (1966).

Balmain, K., "The impedance of a short dipole antenna in a magnetoplasma," IEEE Transactions on Antennas and Propagation Volume AP-12, No. 5 (1964).

Balmain, K., "Impedance of a short dipole in a compressible plasma," Radio Science, 69D (1965).

Balmain, K., "Impedance of radio - frequency plasma probe with an absorptive surface," Radio Science, New Series, 2, No. 1 (1966).

Balmain, K., G. A. Oksiutik, "RF probe admittance in the ionosphere. Theory and experiment," NATO Advanced Study Institute, Norway (1968).

Bernstein, I. B., I. N. Rabinowitz, "Theory of electrostatic probes in a low-density plasma," The Physics of Fluids, 2, No. 2 (1959).

Brown, Sanborn C., "Basic data of plasma physics," John Wiley.

Buckley, R., "A theory of resonance rectification," Proc. Roy. Soc., 290, A, (1966).

Buckley R., "The response of a spherical plasma probe to alternating potentials," J. Plasma Physics, 1, Part 2 (1967).

Bunting, W. D., "Low Frequency Probe Measurements in Laboratory simulated ionosphere plasmas," DASS Internal Report 68-2, Southwest Center for Advanced Studies, (1968).

Cairns, R. B., "Measurements of resonance rectification using a plasma probe," Proc. Phys. Soc., 82, Part 2 (1963).

Crawford, F. W., "Plasma resonance probe characteristic in a magnetic field," J. Appl. Phys., 36, No. 10 (1965).

Crawford, F. W., R. S. Harp, "The resonance probe-A tool for ionospheric and space research," J. Geophys. Res., 70, No. 3 (1965).

Davies, P. G., "The electrical properties of a spherical plasma probe near the plasma frequency," Proc. Phys. Soc., 88, (1966).

Fejer, J. A., "Interaction of an antenna with a hot plasma and the theory of resonance probes," Radio Sci., 68D, No. 11 (1964).

Hall, R. B., "Parallel plate plasma problem," Am. J. Phys., 31, No. 8, (1963).

Harp, R. S., F. W. Crawford, "Characteristics of the plasma resonance probe," J. Appl. Phys., 35, No. 12 (1964).

Heikkila, W. J., "Laboratory study of probe impedance," NATO Advanced Study Institute, Norway (1968).

Heikkila, W. J., J. A. Fejer, J. Hugill and W. Calvert, "Comparison of ionospheric probe techniques," Space Research VII, North-Holland Publishing Co., (1966).

Holt, O., G. M. Lerfald, "Results from an RF capacity probe experiment in the auroral ionosphere," Radio Science, 12, (New Series) No. 11 (1967).

Holt, L., "A note on the effect of collisions on the impedance of a spherical RF plasma probe," Rep. No. E-67, NDRE, Kjeller, Norway (1965).

Kostelnicek, R. J., "An investigation of boundary theories for the resonance probe," Radio Science, 3, (New Series), No. 4 (1968).

Laframboise, J. G., "Theory of spherical and cylindrical langmuir probes in a collisionless, Maxwellian plasma at rest", IAS. University of Toronto, June, 1966.

Mayer, H. M., "Measurements with a wide-band probe," Proc. Intern. Conf. Ionization Phenomena Gases, 6th, Paris, 1963, 4, 129-134, 1964.

Patterson, T. N. L., "The optimum addition of points to quadrature formulae," Mathematics of computation, October, 1968, Volume 22, No. 104.

Pavkovich, J. M., "Numerical calculations related to the RF properties of the plasma sheath," ARF 64-17, Stanford University (1964).

Phelps, A. V., J. L. Pack, "Electron collision frequencies in nitrogen and in the lower ionosphere," Physical Review Letters, 3, No. 7 (1959).

Tarstrup, J., "The impedance characteristic of a spherical plasma probe," DASS Report 68-3, Southwest Center for Advanced Studies (1968).

Wait, J. R., "Theory of a slotted-sphere antenna immersed in a compressible plasma," Radio Sci. J. Res., NBS, 68D, No. 10 (1964).

Wait, J. R., "Electromagnetic and plasmas," Holt, Rinehart and Winston, Inc.

APPENDIX 1

A calculation has been performed to establish if a sufficient sampling volume was obtained for a 1 cm probe located in the center of our vacuum system. The measurements were done in plasmas, where the electron temperature was approximately 350°K and the plasma frequency about 15 MHz. This corresponds to a Debye length of approximately 0.8 mm. Since the radius of the outer screen is 16 cm, at least 150 Debye lengths of plasma are available. In order to simplify the computation, cold plasma theory was used with a gradual sheath profile and a vacuum sheath. Figure 10 shows the density profiles used in the comparison between the impedance characteristic with an infinite uniform plasma and one where the electron density profile is identical to the measured (parabolic) and the plasma is cutoff as 150 λ_D. However, in the measured case, the impedance characteristic is always normalized not to the free space impedance, but to the impedance of the probe to the screen (concentric capacitor). The impedance for a sphere with the given electron density profile can be broken up in three parts in series, the two parts closest to the probe being in common for the two cases. The vacuum part closest to the probe is in effect a concentric spherical capacitor, which impedance can be found from

$$Z_v = \frac{1}{j4\pi\omega\varepsilon_o} \int_{r_o}^{r_1} \frac{dr}{r^2} = \frac{1}{j4\pi\omega\varepsilon_o} \left[\frac{1}{r_o} - \frac{1}{r_1}\right]$$

The transition part from $r = r_1$ to $r = r_2$ is also a concentric spherical capacitor, but the electron density changes from 0 to N. The impedance can be found from

$$Z_t = \frac{1}{j4\pi\omega\varepsilon_o} \int_{r_1}^{r_2} \frac{dr}{r^2 K_o(r)} \qquad \text{where}$$

$$K_o(r) = 1 - \frac{X(r)}{U} \; ; \quad U = 1 - jZ; \; Z = \frac{\nu}{\omega} \; ;$$

$$K_o(r) = 1 - \frac{Ne^2(r-r1)}{m\varepsilon_o \omega^2 U(r_2-r_1)} \qquad \text{or}$$

$$Z_t = \frac{1}{j4\pi\omega\varepsilon_o} \int_{r_1}^{r_2} \frac{dr}{r^2(1-k(r-r_1))} \qquad \text{where}$$

$$k = \frac{X}{U(r_2-r_1)}$$

Finally

$$Z_t = \frac{1}{j\omega 4\pi\varepsilon_o} \left[- \frac{1}{(1+kr_1)} \left(\frac{1}{r_2} - \frac{1}{r_1} \right) - \frac{k}{(1+kr_1)^2} \ln \left(\frac{r_1}{r_2} (1 + kr_1 - kr_2) \right) \right]$$

The impedance from $r = r_2$ to $r = \infty$ for the uniform electron density case can be found from

$$Z_{pl} = \frac{1}{j\omega 4\pi\varepsilon_o} \int_{r_2}^{\infty} \frac{dr}{r^2 K_o} = \frac{1}{j\omega 4\pi\varepsilon_o (1 - \frac{X}{U}) r_2}$$

For the parabolic electron density

$$Z_{P_2} = \frac{1}{j\omega 4\pi\epsilon_o} \int_{r_2}^{r_3} \frac{dr}{r^2 K_o(r)}$$

$$K_o(r) = 1 - \frac{1 - k\,(r-r_2)^2}{U}$$

where $N = N_o\,(1-kr^2)$ from Figure 10

Figure 10 shows the two calculated impedance characteristics. It will be noted that the result is a justification for comparing our experimental results with theoretical models with a uniform electron density. Incidentally, the sheath profile used in above description is similar to one used by Balmain (1969) for a planar probe.

APPENDIX 2

This time the impedance characteristic will be calculated for a probe at space potential. Cold plasma approach is being used with the same justification as stated in Appendix 1. An electron density profile of $N = N_o \frac{r + \sqrt{r^2 - r_o^2}}{2r}$ is assumed, corresponding to the geometric depletion factor due solely to the solid angle subtended by the probe (Laframboise 1966).

$$Z_{probe} = \frac{1}{j\omega 4\pi\varepsilon_o} \int_{r_o}^{\infty} \frac{dr}{r^2 K_o(r)}$$

$$K_o(r) = 1 - \frac{X(r)}{U} \quad ; \quad X(r) = \frac{1}{2r} X \left(r + \sqrt{r^2 - ro^2}\right);$$

The integration (complex) was performed using techniques developed by Patterson (1968) and gave the results that f_r appears approximately 5% below the plasma frequency.

APPENDIX 3

a = absorption coefficient

k = Boltzmann's constant

$K_o = 1 - \frac{X}{U}$

m = electron mass

N = steady ambient electron density

n = oscillating electron density

r = distance from center

r_o = probe radius

s = sheath thickness

T = electron temperature

$U = 1 - J\frac{\nu}{\omega}$

$\bar{v}$ = electron velocity

V = potential

$X = \frac{\omega_N^2}{\omega^2}$

$\alpha = (1 - \frac{U}{X})^{1/2}$

$\alpha_1 = \frac{\alpha}{\gamma^{1/2}}$

γ = ratio of specific heat

ϵ_o = dielectric constant

λ_D = Debye length

ν = collision frequency

$\rho = \frac{r+s}{\lambda_D}$ = normalized sheath radius

ω = frequency

ω_N = plasma frequency

$\chi = \frac{\nu}{\omega_N}$ = normalized collision frequency

C_o = free space probe capacitance

TABLE 1

Probe Size (diameter)	Experiment Number	Frequency Shift of f_r Going From Floating Potential to Space Potential
7 mm	355	+7%
10	138	4
10	171	6
10	185	9
10	228	7
10	233	7
10	324	7
10	346	7
10	424	5
10	427	7
14	144	8
14	164	7
14	193	10
20	305	7
20	311	7

FIGURE CAPTIONS

Figure 1. Experiment arrangement.

Figure 2. Photograph of impedance probe.

Figure 3. Block diagram for measuring the impedance characteristic of a spherical probe.

Figure 4. (a) Phase/amplitude response for a 1 cm probe in a plasma (N_2, 32μ). (b) Phase/amplitude response for the same probe with no plasma in the vacuum chamber.

Figure 5. Normalized electron density profile.

xxoo measured by Langmuir probe techniques

--- theoretical approximation used in Appendix 1.

Figure 6. Experimental impedance characteristics.

. . . probe at floating potential

xxx probe at space potential

Figure 7. Theoretical imepdance characteristics.

_____ hydrodynamic approach with density profile A

xxx hydrodynamic approach with density profile B

_____ – cold plasma approach with density profile A

ooo cold plasma approach with density profile B

Figure 8. Theoretical impedance characteristics.

_____ Buckley $r_o = 5.2\ \lambda_D$; $\chi = 0.05$

---- Buckley $r_o = 5.2\ \lambda_D$; $\chi = 0.15$

_____ – Hydrodynamic $r_o = 6\ \lambda_D$; $\chi = 0.35$; $s = 4\lambda_D$

Figure 9. Impedance characteristics.

. . . experimental points at floating potential

xxx experimental points at space potential

——— theoretical hydrodynamic $r_o = 6\lambda_D$; $\chi = 0.35$; $s = 4.3\lambda_D$

——— — theoretical hydrodynamic $r_o = 6\lambda_D$; $\chi = 0.35$; $s = 0$

Figure 10. Theoretical impedance characteristics.

——— cold plasma approach with density profile A

. . . cold plasma approach with density profile B

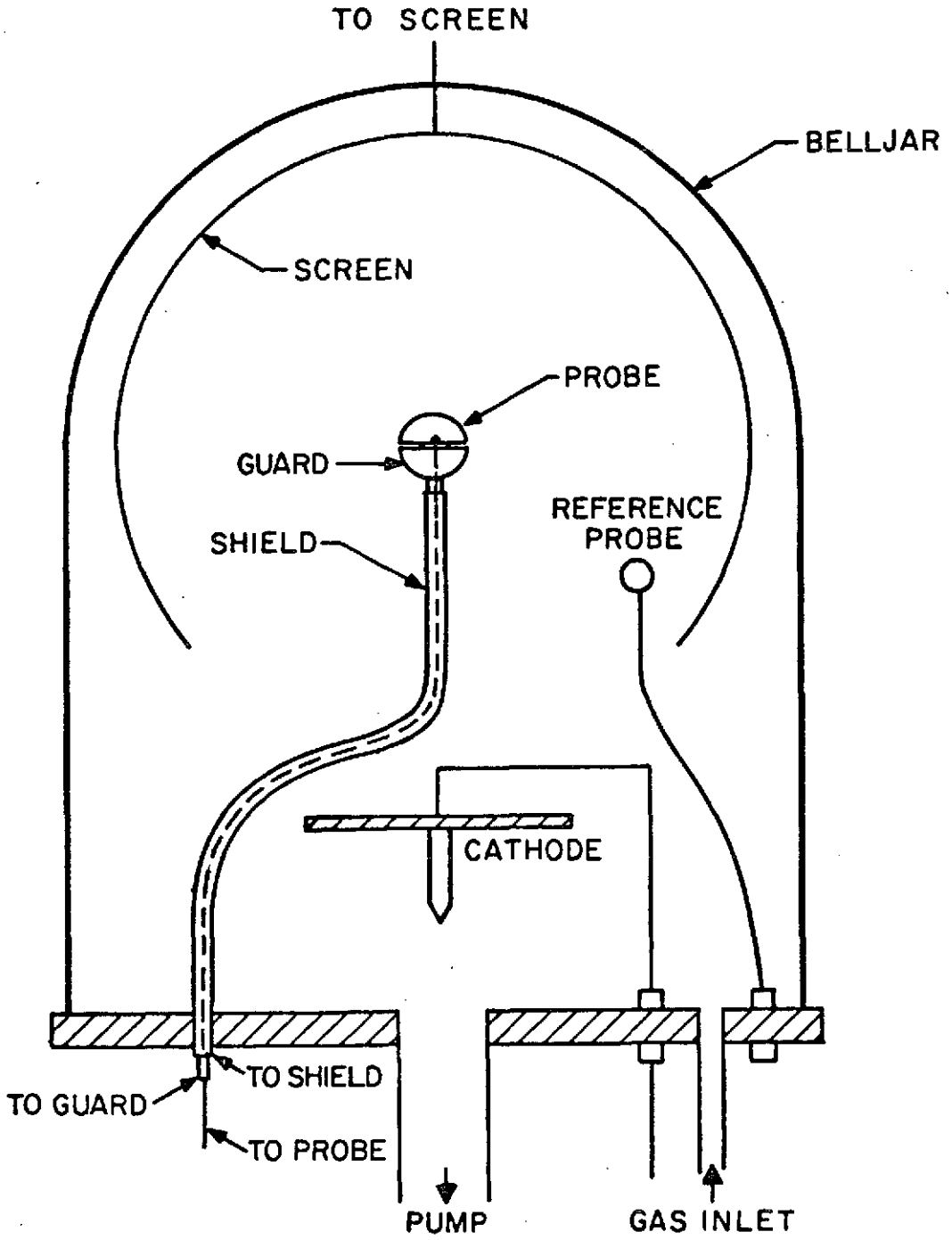
TO SCREEN
BELLJAR
SCREEN
PROBE
GUARD
SHIELD
REFERENCE PROBE
CATHODE
TO SHIELD
TO GUARD
TO PROBE
PUMP
GAS INLET

FIGURE 1

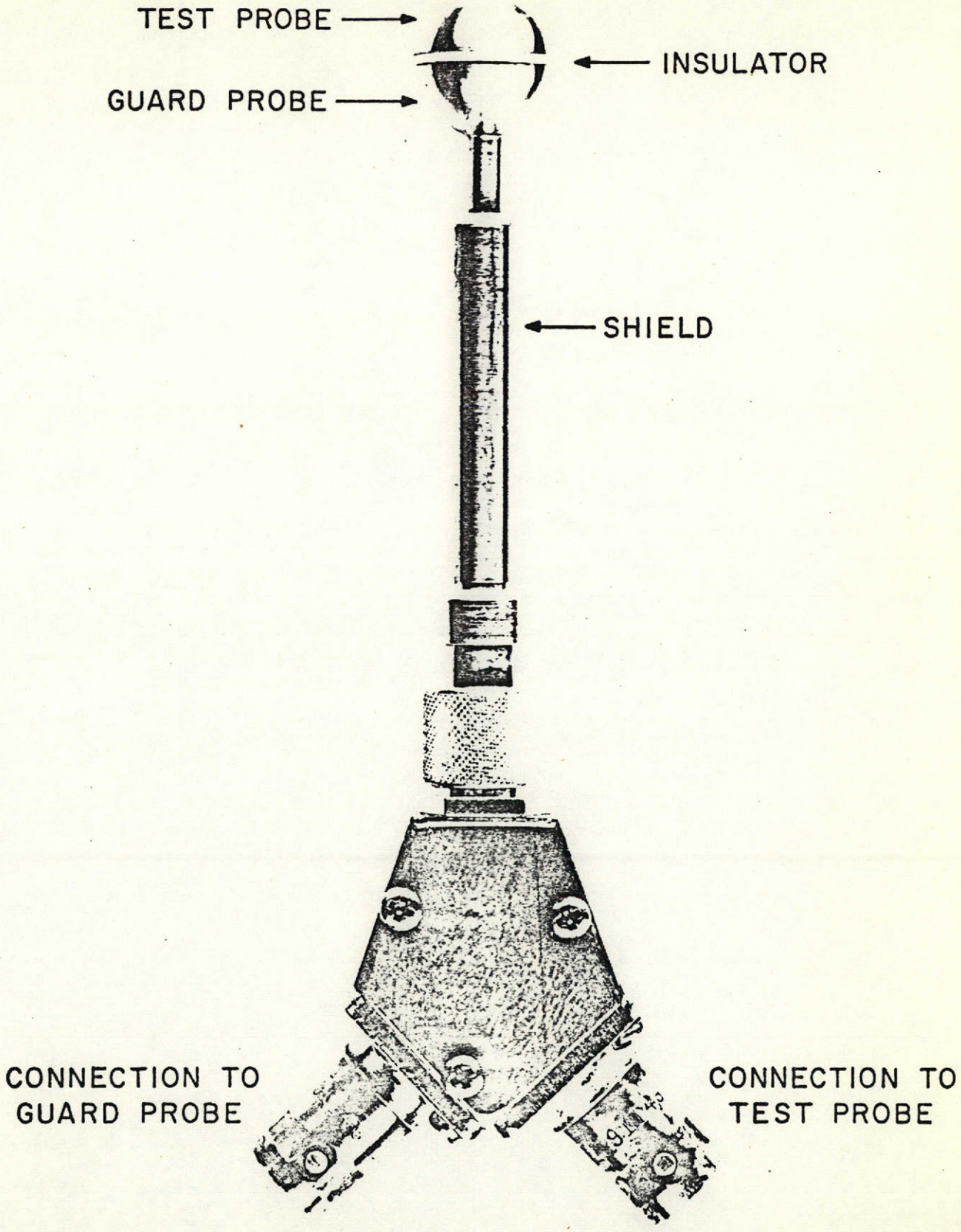
TEST PROBE
GUARD PROBE
INSULATOR
SHIELD
CONNECTION TO GUARD PROBE
CONNECTION TO TEST PROBE

FIGURE 2

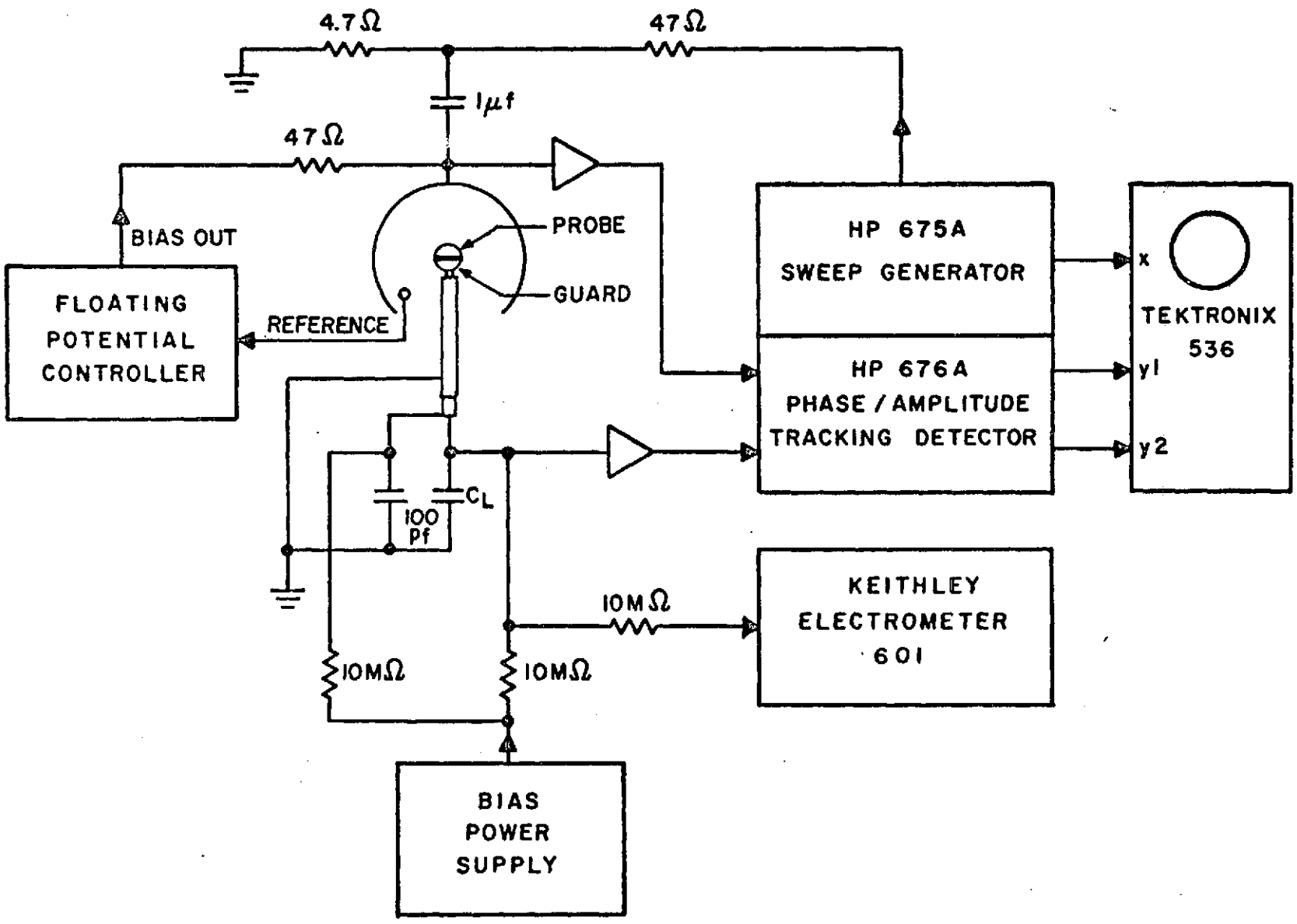
4.7Ω
47Ω
1μf
47Ω
BIAS OUT
PROBE
GUARD
FLOATING POTENTIAL CONTROLLER
REFERENCE
HP 675A SWEEP GENERATOR
HP 676A PHASE / AMPLITUDE TRACKING DETECTOR
TEKTRONIX 536
x
y1
y2
100 Pf
C_L
10MΩ
10MΩ
10MΩ
KEITHLEY ELECTROMETER 601
BIAS POWER SUPPLY

-29-

FIGURE 3

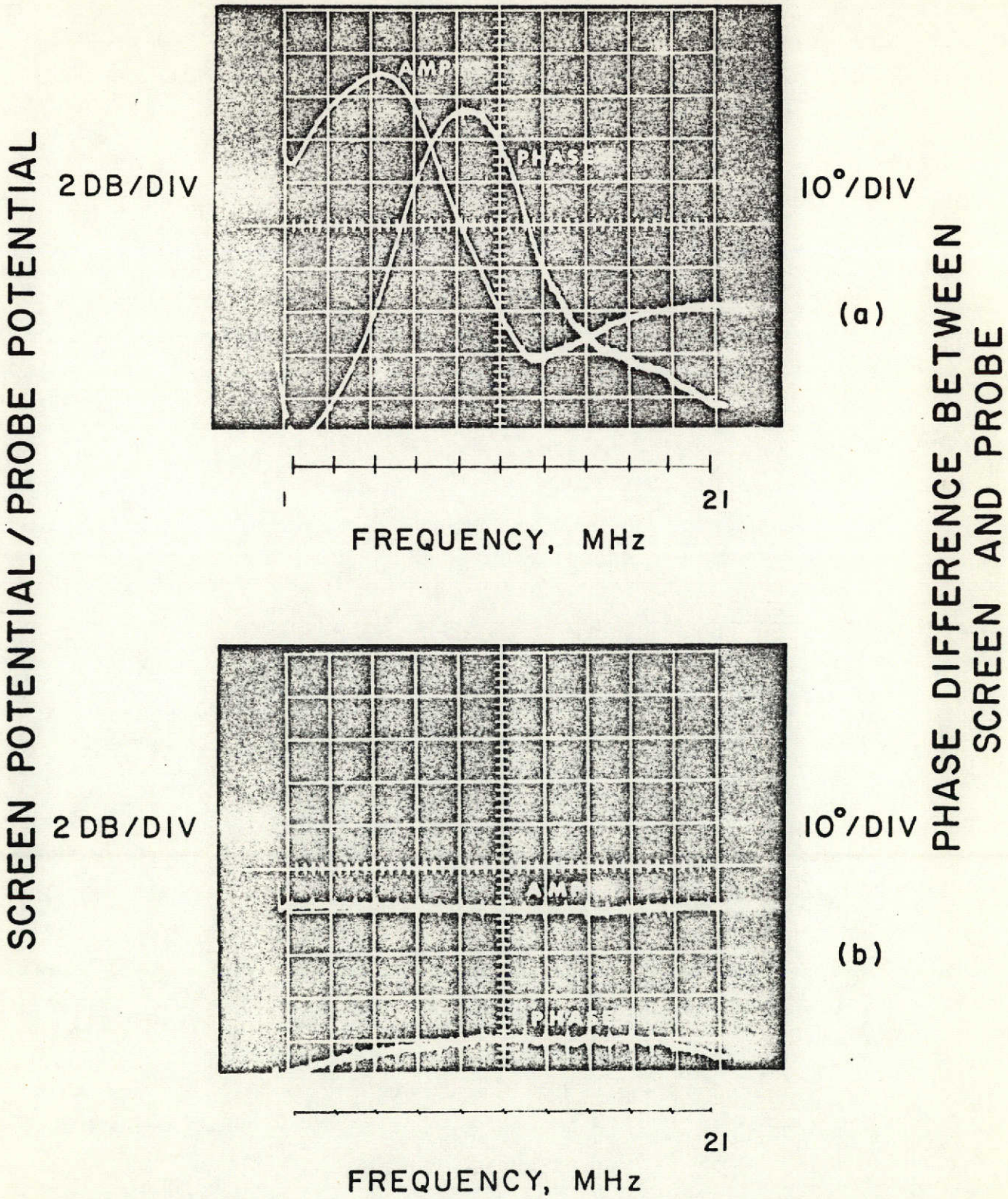
SCREEN POTENTIAL / PROBE POTENTIAL
2 DB/DIV
AMP
PHASE
10°/DIV
(a)
PHASE DIFFERENCE BETWEEN SCREEN AND PROBE
1
21
FREQUENCY, MHz
2 DB/DIV
10°/DIV
(b)
21
FREQUENCY, MHz

FIGURE 4

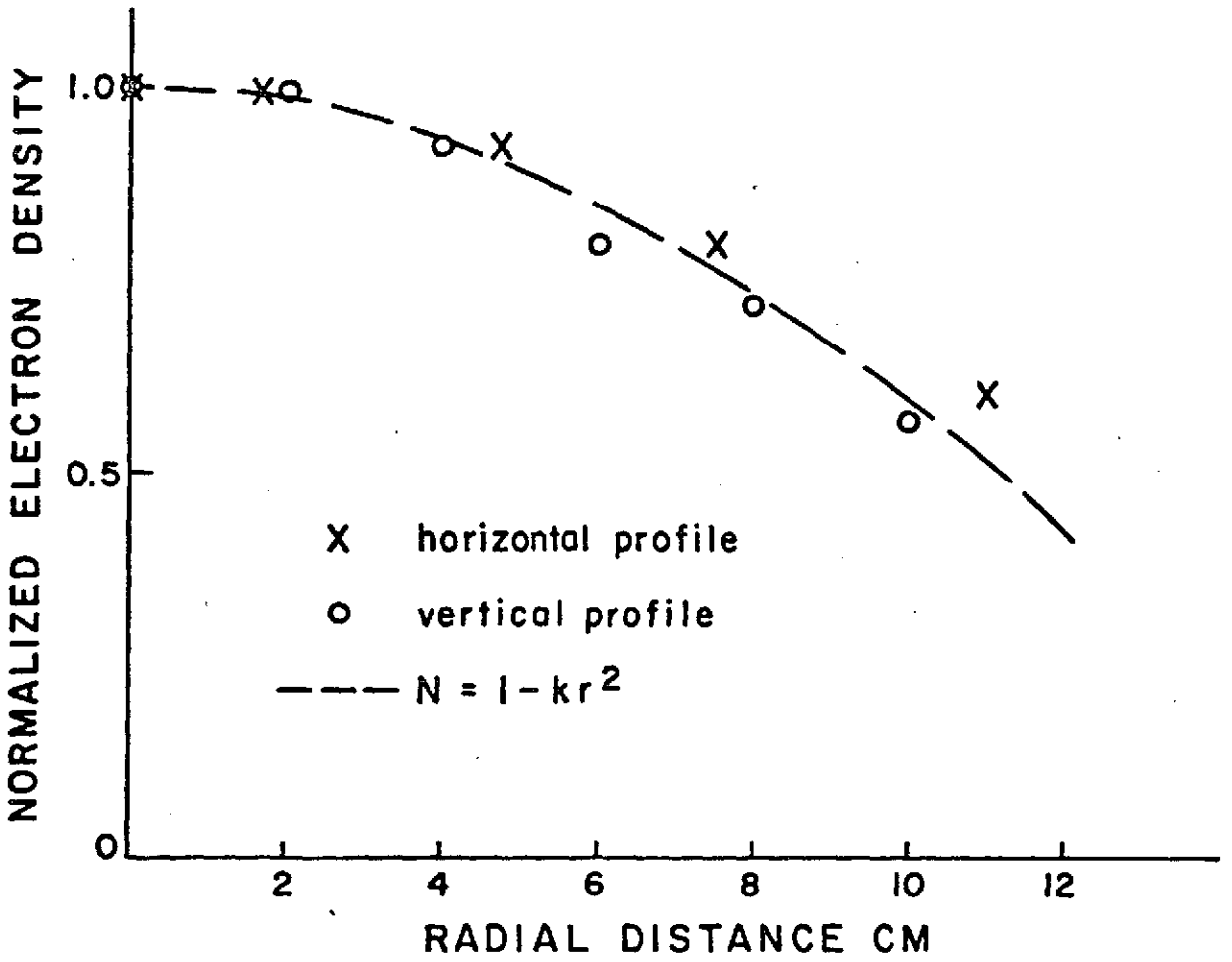
NORMALIZED ELECTRON DENSITY
1.0
0.5
0
2
4
6
8
10
12
RADIAL DISTANCE CM
X horizontal profile
O vertical profile
N = 1 - kr²

FIGURE 5

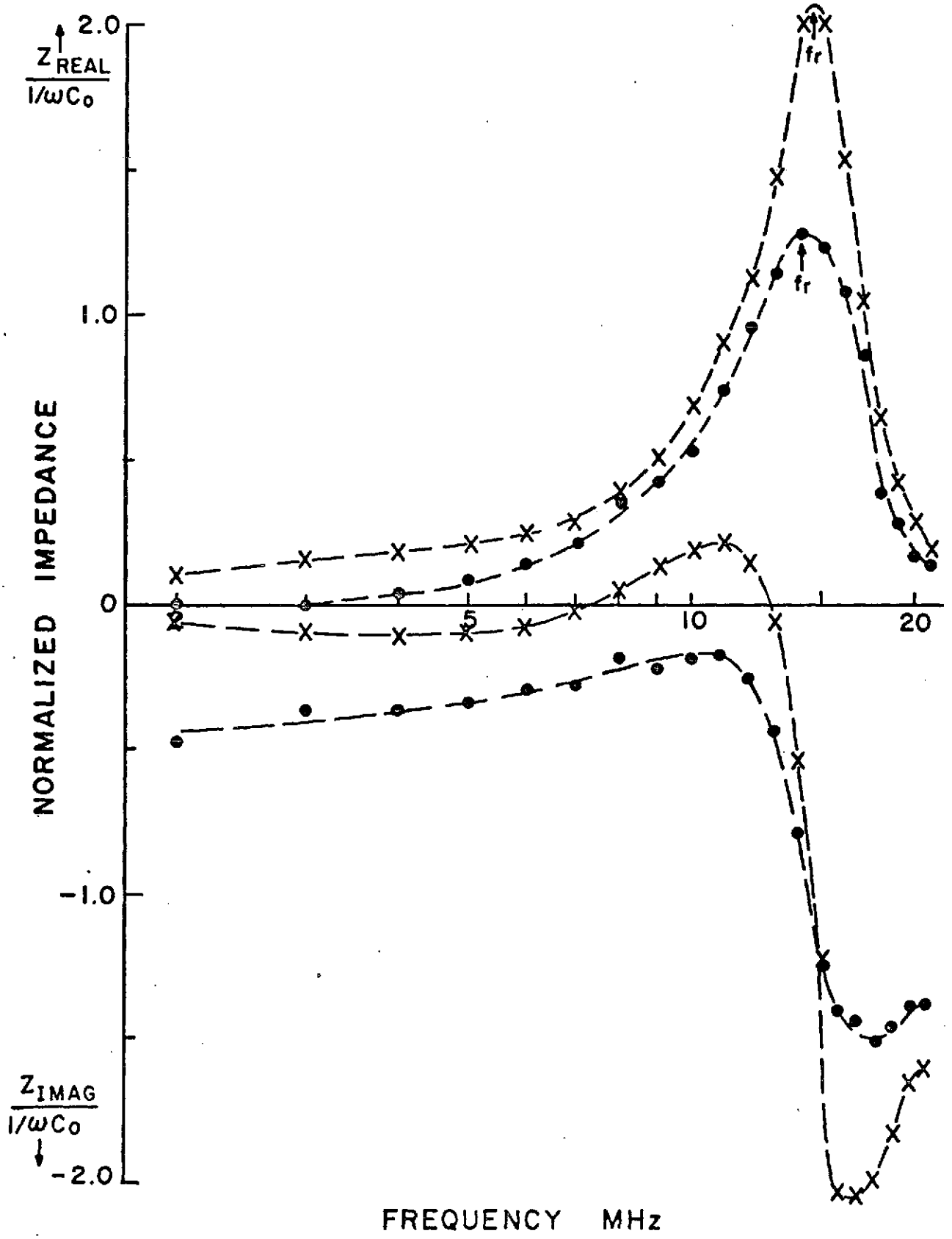
2.0
Z_{REAL} / $1/\omega C_o$
1.0
0
-1.0
Z_{IMAG} / $1/\omega C_o$
-2.0
NORMALIZED IMPEDANCE
5
10
20
f_r
f_r
FREQUENCY MHz

FIGURE 6

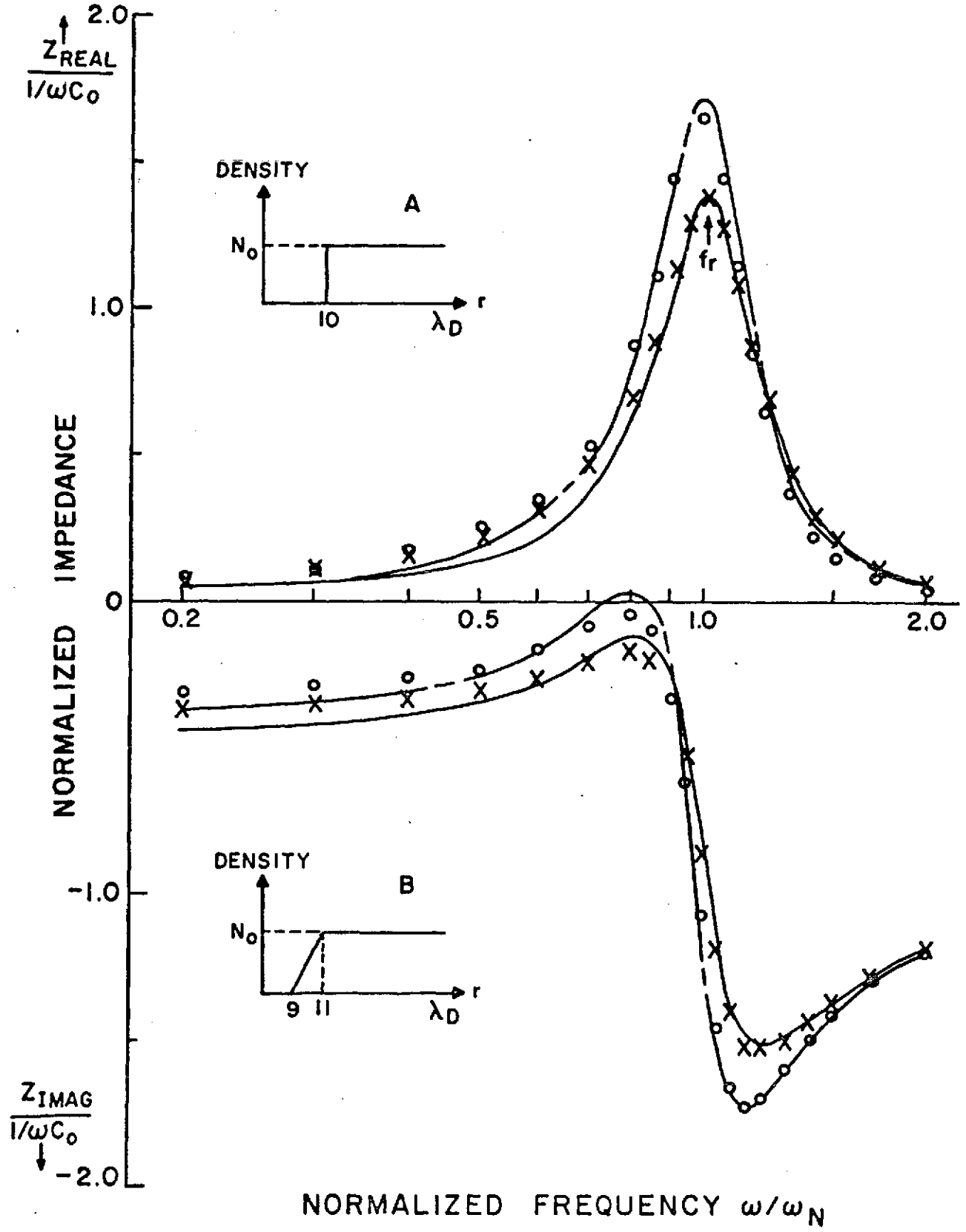
2.0
Z_{REAL}
$1/\omega C_o$
1.0
0
-1.0
Z_{IMAG}
$1/\omega C_o$
-2.0
NORMALIZED IMPEDANCE
DENSITY
A
N_o
10
r
λ_D
f_r
0.2
0.5
1.0
2.0
DENSITY
B
N_o
9
11
r
λ_D
NORMALIZED FREQUENCY ω/ω_N

FIGURE 7

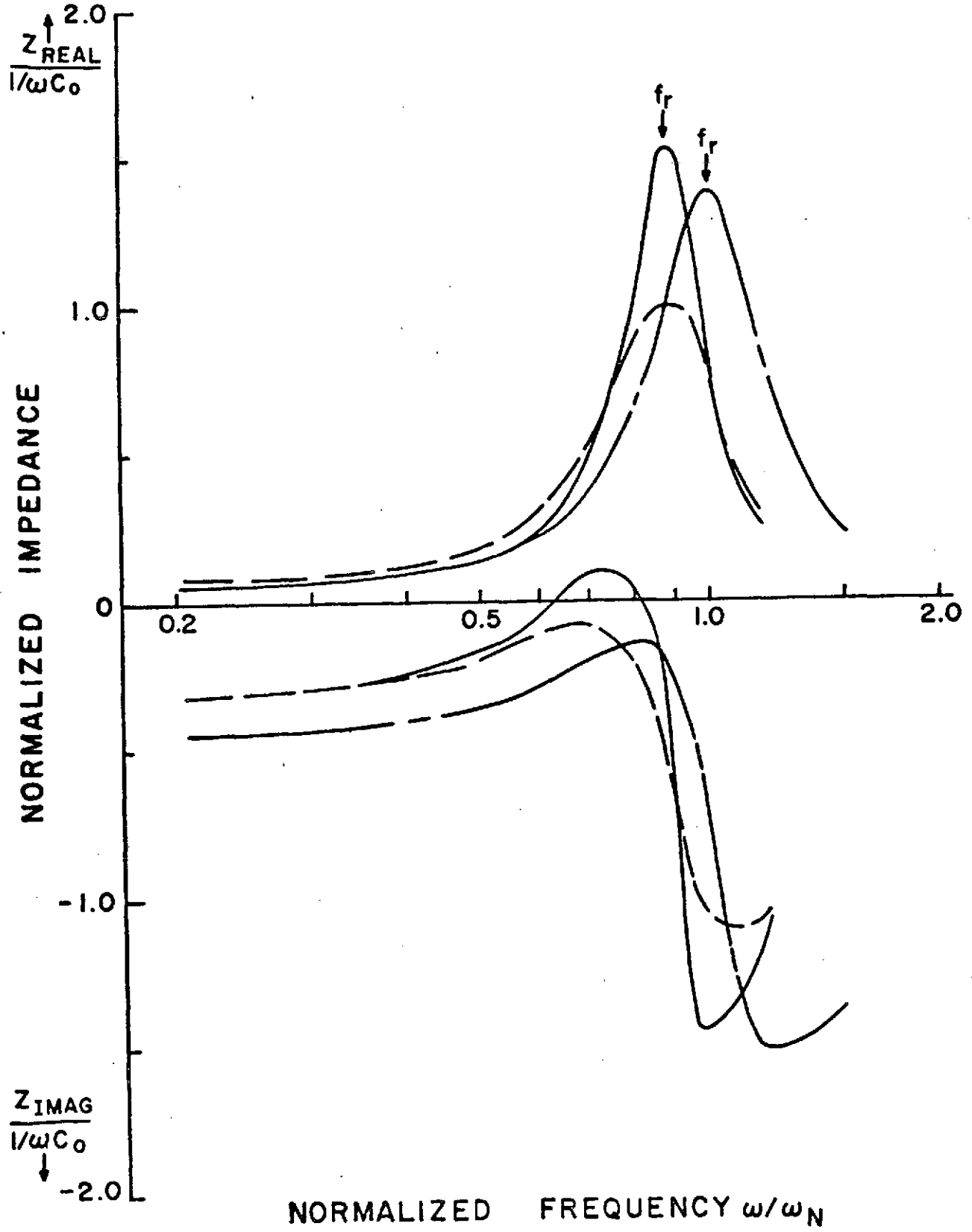
2.0
Z_{REAL} / $1/\omega C_o$
1.0
0
-1.0
Z_{IMAG} / $1/\omega C_o$
-2.0
NORMALIZED IMPEDANCE
f_r
f_r
0.2
0.5
1.0
2.0
NORMALIZED FREQUENCY ω/ω_N

FIGURE 8

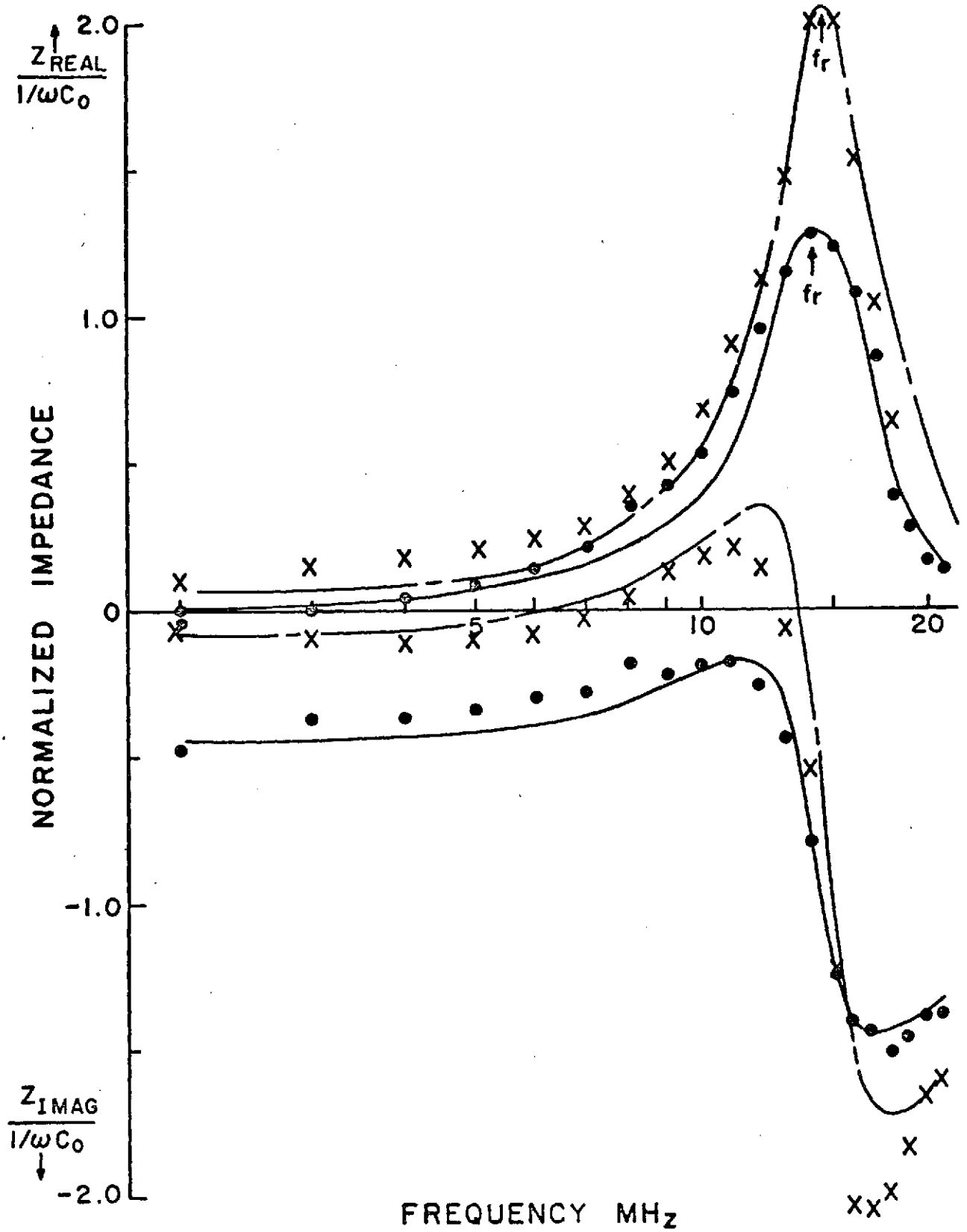
2.0
Z_{REAL} / $1/\omega C_o$
1.0
0
-1.0
Z_{IMAG} / $1/\omega C_o$
-2.0
NORMALIZED IMPEDANCE
f_r
f_r
5
10
20
FREQUENCY MHz

FIGURE 9

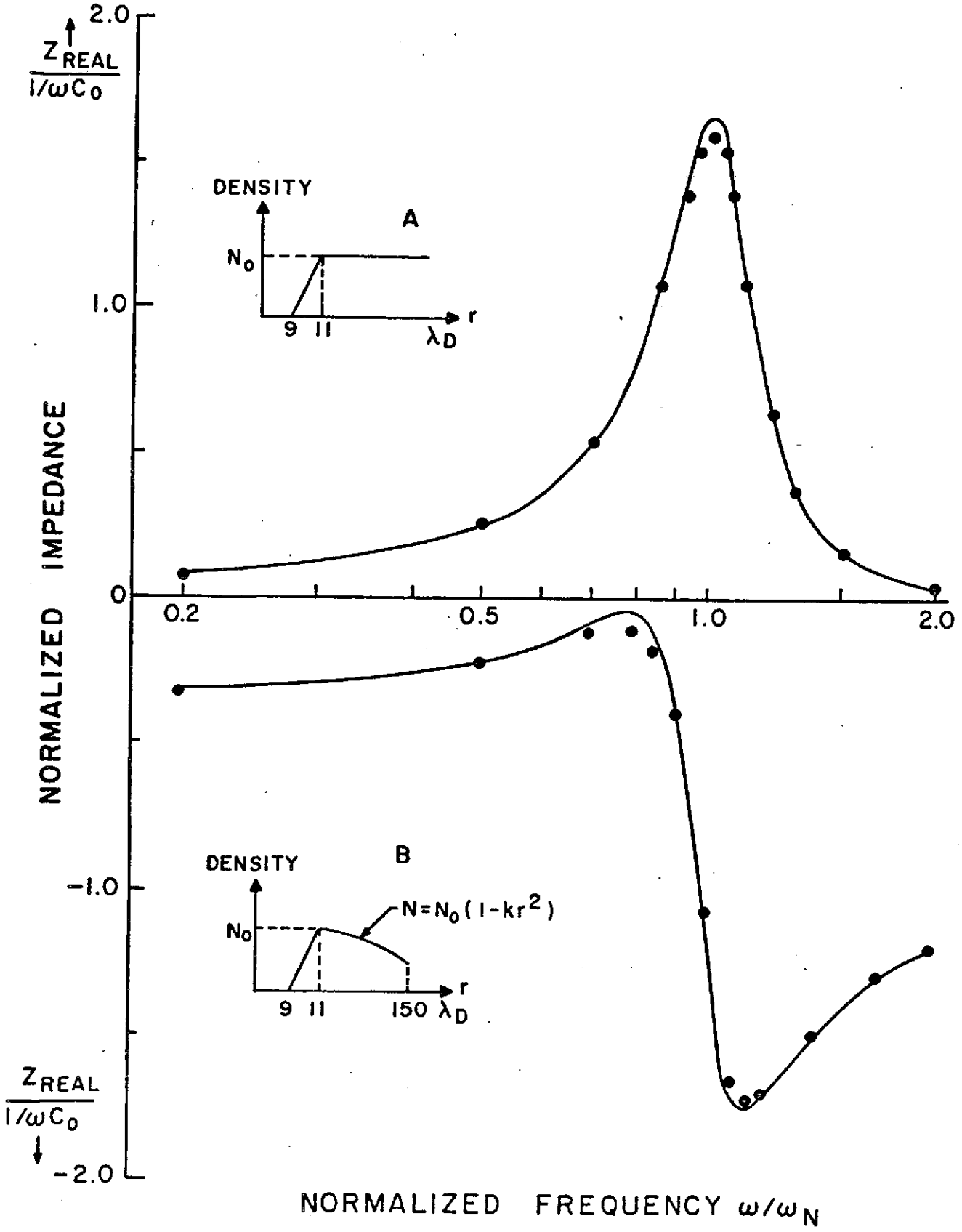
2.0
Z_{REAL}
$1/\omega C_0$
1.0
0
-1.0
Z_{REAL}
$1/\omega C_0$
-2.0
NORMALIZED IMPEDANCE
DENSITY
A
N_0
9
11
r
λ_D
0.2
0.5
1.0
2.0
DENSITY
B
$N=N_0(1-kr^2)$
N_0
9
11
150
r
λ_D
NORMALIZED FREQUENCY ω/ω_N

FIGURE 10